Magnetism of ultrathin $Pd_{99}Fe_{01}$ films grown on niobium

2014 Mater. Res. Express 1 036104

(http://iopscience.iop.org/2053-1591/1/3/036104)

Materials Research
Express

Magnetism of ultrathin $Pd_{99}Fe_{01}$ films grown on niobium

L S Uspenskaya[1], **A L Rakhmanov**[2,3], **L A Dorosinskii**[4], **S I Bozhko**[1], **V S Stolyarov**[1,5] **and V V Bolginov**[1]

[1] Institute of Solid State Physics RAS, Chernogolovka, 142432, Russia
[2] Institute for Theoretical and Applied Electrodynamics, RAS, Moscow, 125412 Russia
[3] Moscow Institute of Physics and Technology (State University), Dolgoprudnyi, Moscow Region, 141700 Russia
[4] National Institute of Metrology (TUBITAK-UME), P.K. 54, 41470, Gebze-Kocaeli, Turkey
[5] CNRS, UMR 7588, Institut des Nanosciences de Paris, F-75005 Paris, France
E-mail: uspenska@issp.ac.ru

Received 14 May 2014, revised 24 June 2014
Accepted for publication 3 July 2014
Published 22 July 2014

Materials Research Express **1** (2014) 036104

doi:10.1088/2053-1591/1/3/036104

Abstract

Magnetic properties of ultrathin $Pd_{99}Fe_{01}$ films grown on niobium films are investigated by magneto-optic visualization, SQUID magnetometry, and Hall-voltage measurements in the temperature range from 3 to 40 K. We show that the films are ferromagnetic at thickness larger than 10 nm. The Curie temperature T_C varies from 2 to 40 K with increase of film thickness to 80 nm. The value of spontaneous magnetization of the $Pd_{99}Fe_{01}$ depends on the PdFe film thickness. The estimated spin polarization is about $4\,\mu_B$ per Fe ion, which corresponds to the polarization of the Pd_3Fe compound. In contrast to the homogenous bulk material, $Pd_{99}Fe_{01}$ films consist of ferromagnetic nano-clusters in a paramagnetic host, which is confirmed by characteristic features of the magnetization loops and by the increase of critical current density in the adjacent Nb layer. The size of the clusters is estimated as 10 nm, which is in agreement with the 30% increase of the supercurrent observed in the Nb.

Keywords: PdFe alloy, magnetic structure, magnetization, hysteresis, nanoclusters

1. Introduction

Diluted alloy $Pd_{1-x}Fe_x$ is a weak ferromagnet with prospective use in superconductor–ferromagnet–superconductor (SFS) structures [1–4]. A weak ferromagnet with easily rotated magnetization allows one to control current in the SFS structures by application of a small

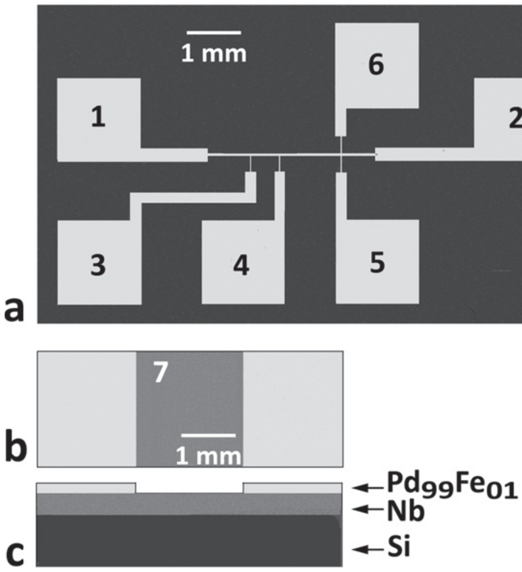

Figure 1. Sketches of the samples. (a) Bilayer sample for standard four-probe resistance and Hall voltage measurements fabricated on the Si substrate: 1 and 2—current contacts; 3 and 4—potential contacts to measure resistivity; 5 and 6—contacts to measure Hall voltage. (b), (c) Planar and side views of the sample for visualization of the magnetization reversal process. Note that the Nb layer is covered by the $Pd_{99}Fe_{01}$ film on the sample edges, while the center part of the sample (marked by 7) is naked.

magnetic field [5–7]. In the SFS systems the ferromagnetic layer should be thin to ensure the link between the superconducting layers. The properties of bulk $Pd_{1-x}Fe_x$ alloys have been studied in detail [8–14], while only a few papers are devoted to thin films [4, 15, 16]. The properties of thin films are sensitive to film thickness and substrate. The proximity effect and distortion of the magnetic field distribution by the superconducting layers could also affect the characteristics of the SFS structure.

In this paper we study the magnetic properties of ultrathin $Pd_{99}Fe_{01}$ films deposited on the Nb films. We observe that $Pd_{99}Fe_{01}$ films are ferromagnetic if their thickness is greater than 10 nm. We show that the $Pd_{99}Fe_{01}$ films consist of ferromagnetic nano-clusters in a paramagnetic host. The material is magnetically soft and one can expect a high rate of dynamic magnetization reversal. The non-homogeneous magnetization of the neighboring ferromagnetic film gives rise to an increase of the effective pinning of Abrikosov vortices in the Nb film, and as a result to the growth of the critical supercurrent density.

2. Experiment

The experiments were performed on bilayer PdFe–Nb hybrid films. Both metallic layers were fabricated in a single vacuum cycle. The lower Nb layer with the thickness of $D = 100$ nm was deposited by dc magnetron sputtering on a 5×15 mm^2 Si substrate. The upper PdFe layer with the thickness d of 10–80 nm was deposited by rf magnetron sputtering. The films were patterned by lift-off lithography for resistive and Hall voltage measurements and for visualization of the magnetization reversal process as shown in figures 1(a)–(c).

The superconducting transition temperature T_C of Nb measured by the four-probe method was found to be about 8.6 K with a transition width of 0.5 K. These values were independent of the presence and thickness of the PdFe layer within the experimental accuracy (about 0.2 K). The critical current density j_c of the Nb film measured by the four-probe technique was about 4×10^5 A cm^{-2} at $T = 7$ K.

The Curie temperature T_C of the ferromagnetic PdFe layer was extracted from Hall voltage dependences on the magnetic field and temperature, $V(H, T)$. The measurements are based on the Hall effect sensitivity to magnetic scattering, which occurs due to the spin–orbit coupling [17]. In ferromagnetic materials, the Hall voltage varies fast at low magnetic field when the magnetic domains order. With further field increase, the Hall voltage grows linearly, corresponding to the ordinary Hall effect [18–21]. The dependence of $V(H, T)$ may be described as $V(H, T) \propto B(H, T) = H + 4\pi M(H, T)$ [20, 21]. The extrapolation of $B(H, T)$ to zero H gives the voltage $V_H(T)$, which is proportional to $4\pi M(T)$. Therefore, T_C can be determined from $V_H(T)$ in the same manner as from $M(T)$, namely as the inflection point of the $V_H(T)$. The method is usually applied as an express method to determine the T_C of weak ferromagnet materials [7, 19].

Complementary measurements of $M(T)$ were made by standard SQUID magnetometry, mainly to check the applicability of the Hall method for our samples. Hysteresis loops and magnetic susceptibilities of some samples were also measured by the SQUID.

To study the magnetization reversal process and the influence of PdFe layers on superconducting properties of the Nb layer, the magneto-optic (MO) visualization technique with an external indicator film was applied. For this purpose, a thin yttrium–iron garnet film was superimposed on the top surface of the sample. The map of the distribution of the perpendicular component of the induction $B_z(x, y)$ was registered by SDU285 digital video camera. This map was used to recover the induction inside the sample and current distribution in the superconducting layer [22, 23].

For the immediate comparison of the properties of a single niobium layer and that covered with the PdFe, the bilayer Nb–PdFe samples with uncovered niobium in the center part were fabricated by reactive ion etching (figures 1(b) and (c)).

The topography of the surfaces of Nb and PdFe grown on the Nb was studied by standard atomic-force microscopy on the same samples.

3. Results

A typical dependence of the Hall voltage $V(H)$ on the applied transverse magnetic field H is shown in figure 2(a) for three different temperatures. At low fields and temperatures, the functions $V(H)$ are nonlinear with a small hysteresis (a few oersted when the applied field is swapped between ±1.5 kOe). The function $V(H)$ is linear if H is large enough. We extrapolate this linear dependence to $H = 0$ and obtain the value V_H, which characterizes the non-linearity of the Hall voltage $V(H)$ at given temperature. The measured variation of V_H with T is given in figure 2(b). The inflection point of $V_H(T)$ is taken as T_C (an explanation of the procedure is given in the 'Experiment' section).

The T_C found by Hall measurements is in reasonable agreement with the ferromagnetic transition temperature obtained from the dependence of magnetization on temperature $M(T)$ measured by the SQUID magnetometer (figure 3(a)). The magnetization decreases with

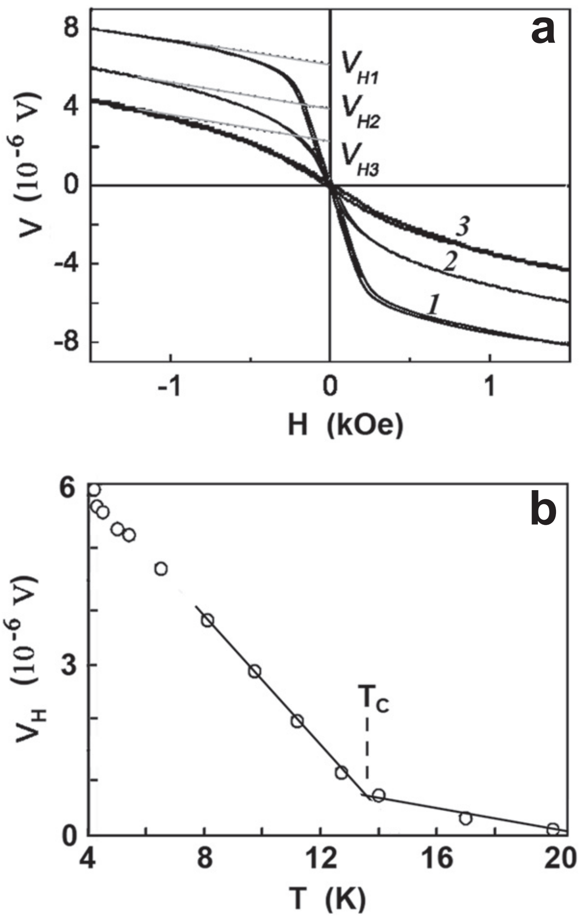

Figure 2. (a) The dependence of Hall voltage on the applied transverse magnetic field for different temperatures: 1—T = 4.2 K, 2—9.7 K, and 3—12.2 K; the thickness of the PdFe film is 40 nm. (b) The dependence of V_H (which characterizes the Hall voltage non-linearity) on temperature.

temperature, which is typical for ferromagnetic materials. However, the transition to the paramagnetic state is not sharp. Moreover, the temperature of the transition shifts towards higher values with increase of the applied magnetic field. If $H < 5$ Oe, the transition occurs near T = 14 K, which is in agreement with the Hall measurements. If the temperature is fixed, the value of magnetization depends on the applied field and does not saturate even if $H >$ 1–2 KOe. For example, if T = 3 K, $M = 3.6 \times 10^{-6}$ emu in the field H = 1.5 Oe and $M_{\max} = 4.2 \times 10^{-6}$ emu in the field H = 50 Oe. The observed smooth magnetic transition, as well as the magnetization variation under the magnetic field, is typical for granular systems due to scattering in the sizes of magnetic grains.

The temperature dependence of the low-frequency magnetic permeability $\mu(T)$ is shown in figure 3(b). An abrupt drop of $\mu(T)$ to a negative value at $T \approx 9$ K occurs due to the transition of the Nb layer to the superconducting state. A slow decrease of $\mu(T)$ with growth of T corresponds to the behavior of $M(T)$ shown in figure 3(a). The permeability $\mu(T)$ depends on the frequency (see figures 3(b) and (c)). For example, variation of the frequency from 1 to 1000 Hz shifts the temperature $T_{\max}$ at which the maximum of permeability is achieved by about

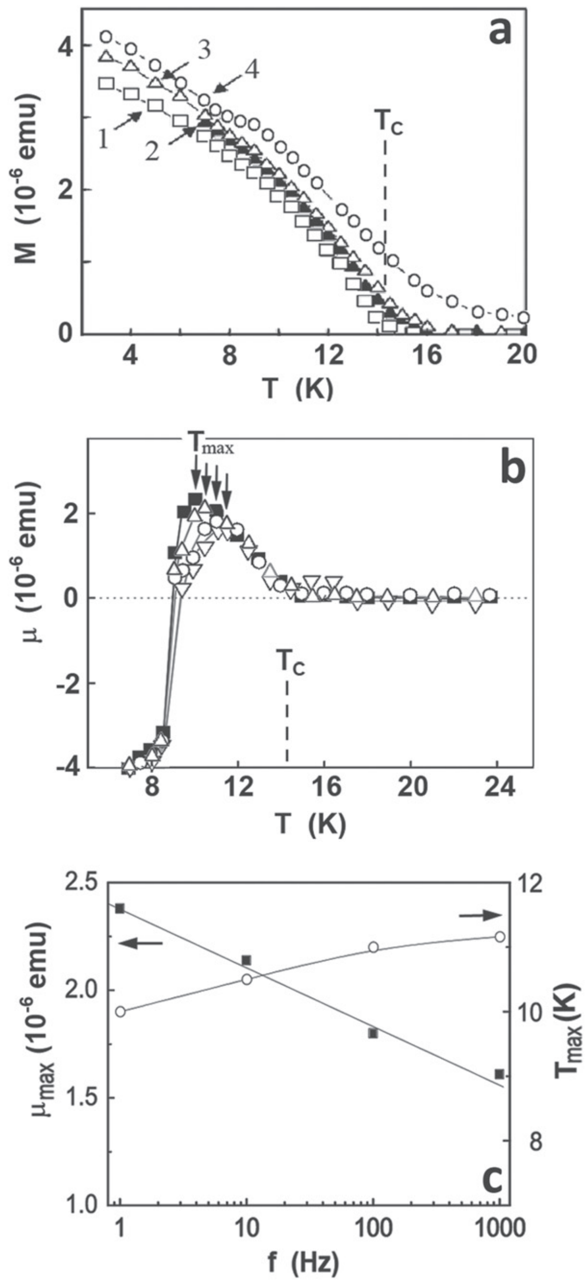

Figure 3. (a) Dependence of magnetization M on T in different applied magnetic fields: 1—H = 1.5 Oe, 2—5 Oe, 3—10 Oe, and 4—50 Oe. The magnetic field H is applied in the film plane; the thickness of the PdFe film is 40 nm. (b) The dependence of the magnetic permeability μ on temperature. The measurements are made in the ac magnetic field with frequency 1 Hz (squares), 10 Hz (down triangles), 100 Hz (circles), and 1000 Hz (up triangles). Note that the maxima of the curves $\mu(H)$ shift toward higher temperature with the increase of frequency as shown below. (c) The dependences of μ_{max} (black squares, left panel) and T_{max} (open circles, right panel) on frequency.

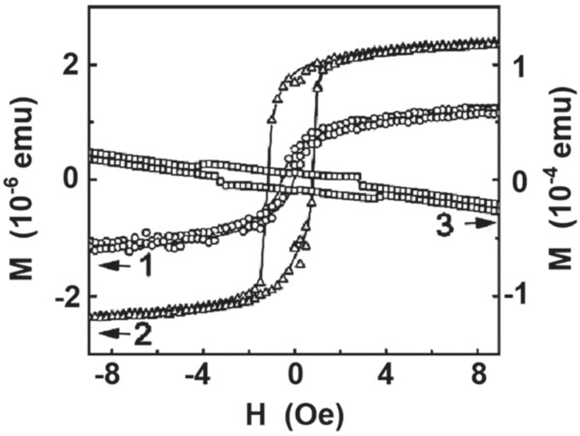

Figure 4. Hysteresis loops at different temperatures: 1—T = 13 K, 2—10 K, 3—4 K (right and left scales differ by two orders of magnitude). The magnetic field is applied in the film plane. The sample is the same as in figure 3.

20% and reduces the maximum value of the permeability μ_{max} by about 30%. Naturally, the frequency does not affect the Curie temperature. The permeability measurements confirm the conclusion that the superconducting critical temperature of the Nb film practically does not depend on the presence or absence of the PdFe cover. The possible reason for this fact is considered in the discussion.

The hysteresis loops $M(H)$ are shown in figure 4 (the field H is applied in the film plane). If the temperature is higher than the superconducting transition temperature of Nb, $T > T_C$, the loops have two distinct parts. The first part is a steep magnetization in the field $H < 2$ Oe and the second one is a smooth approach to saturation at higher fields. However, the saturation is not achieved even if the field is higher than 1 KOe. The coercivity $H_c(T)$ increases with the decrease of temperature: $H_c(13\text{ K}) = 0.5$ Oe, $H_c(10\text{ K}) = 1$ Oe, and $H_c(5\text{ K}) = 3$ Oe. The appearance of the hysteresis loops such as curves 1 and 2 in figure 4 is typical for a nano-granular ferromagnet with weakly interacting grains [24, 25].

The MO visualization of the magnetization reversal of hybrid PdFe-Nb bilayer films was performed in both in-plane and transverse magnetic fields. The MO imaging shows that the magnetic flux is concentrated near the sample edges in the in-plane field in the temperature range $9 < T < 14$ K. This indicates that the magnetic permeability of the sample is higher than vacuum permeability, which is in agreement with the Hall and SQUID magnetometry data. The MO images observed in the in-plane applied field are independent of the field direction, and the residual magnetization is directed along the applied field. No traces of magnetic domain walls are observed. The density of the magnetic flux near the sample edges is approximately proportional to the strength of the applied in-plane field. All these features are characteristic of granular ferromagnetic films with weakly interacting grains [24].

If the temperature is below the superconducting critical temperature of the Nb film $T_c \approx 8.6$ K, the transverse magnetic field is screened by the supercurrent. When this field exceeds some threshold value, the magnetic flux starts to penetrate the sample. The flux distribution has a shape typical for a superconducting plate (figure 5). The MO images in figure 5 show that the flux penetration into the Nb area covered by PdFe is less than in the PdFe free area by about 30%. This means that the presence of the PdFe layer gives rise to an increase

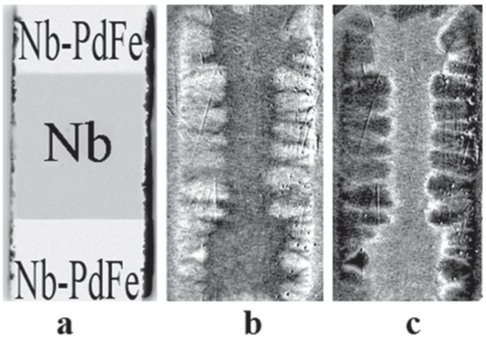

Figure 5. Penetration of the transverse magnetic flux into hybrid Nb–PdFe structure at $T = 7\,K$: (a) view of the sample surface (sample width is 1.8 mm); (b), (c) flux distribution in the transverse field +14.4 Oe and −14.4 Oe, respectively. The depth of the flux penetration to the Nb area covered by PdFe is less than in the PdFe-free region. The thickness of the PdFe layer is 40 nm.

of the supercurrent density. We believe that the cluster magnetic structure of the PdFe film causes an increase of the magnetic flux pinning in Nb and, as a result, the growth of the screening current density. Thus, the deposition of PdFe on the Nb film increases the critical current density.

4. Discussion

The obtained results clearly indicate that the $Pd_{0.99}Fe_{0.01}$ films have a nano-cluster magnetic structure. The characteristic size of the magnetic cluster could be estimated using the concentration of Fe ions in the film and magnetization measured at the lowest temperature (3 K), when the magnetic moment polarization of the ions is maximum. Taking for estimates $M\,(3\ K) = 4 \times 10^{-6}$ emu, we obtain that the magnetization per unit volume is $m = 23.2$ emu cm^{-3}. Palladium has a face-centered cubic lattice with a lattice constant $a = 0.389$ nm. Then, we find that 1 cm^3 of $Pd_{0.99}Fe_{0.01}$ alloy contains 6.8×10^{20} ions of Fe and each Fe ion has an effective magnetic moment of about 3.7 μ_B. This value is close to the 4 μ_B corresponding to the compound Pd_3Fe [26].

The alloy $Pd_{0.99}Fe_{0.01}$ is paramagnetic if localized magnetic moments of 4 μ_B are randomly distributed in it [27]. Thus, we have to suggest that atomic magnetic moments form clusters. The ferromagnetism in PdFe grains disappears if the grain sizes are smaller than 10 nm [28]. This fact is in agreement with our data shown in figure 6, where the dependence of T_C in our samples is shown as a function of the film thickness d. The value of T_C tends to zero if $d \lesssim 10$ nm. Thus, we conclude that the characteristic size r_g of the magnetic nano-clusters in our films is not less than 10 nm, while the characteristic distance l_g between these clusters is not less than 100 nm.

The atomic force microscope image of the surface of the $Pd_{0.99}Fe_{0.01}$ film, its fast Fourier transformation, and the surface roughness are shown in figure 7. For comparison, the surface of the niobium sublayer is given too. One can see that the $Pd_{0.99}Fe_{0.01}$ films are polycrystalline with the average distance between the centers of large grains being about 125 nm. According to our previous estimate each such grain must contain a ferromagnetic cluster. Following [28], it is reasonable to suggest that the ferromagnetic cluster is located near the grain center while the

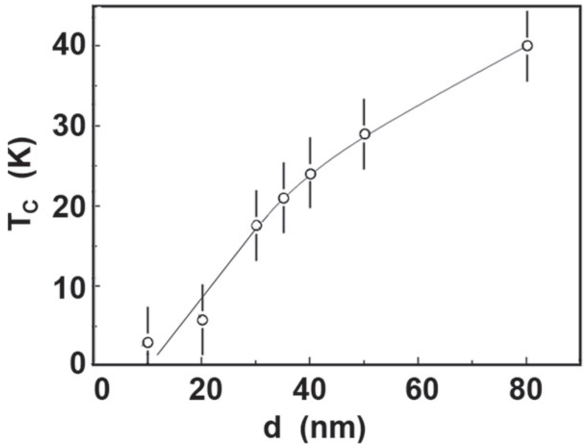

Figure 6. Dependence of T_C of the $Pd_{0.99}Fe_{0.01}$ films on the film thickness d.

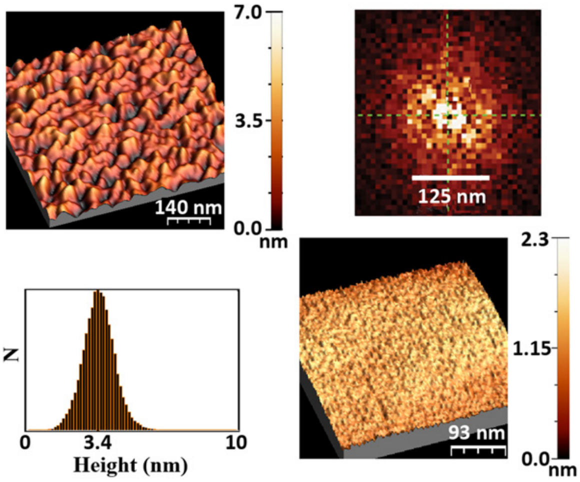

Figure 7. Atomic force microscope image of the top surface of a PdFe film grown on Nb (top left panel), the fast Fourier transformation of the image (top right panel), the result of the surface roughness analysis (bottom left panel), and the image of the surface of single-layer Nb (bottom right panel).

grain shell is paramagnetic. Based on these observations we arrive at estimates of $r_g \sim 10\,\mathrm{nm}$ and $l_g \sim 100\,\mathrm{nm}$.

Inhomogeneous nano-cluster structure of the magnetic layer is a possible reason for the increase of magnetic flux pinning in the superconducting layer and the growth of the critical current density [29]. The magnetic induction in the ferromagnetic film $\mathbf{B}$ is the sum of the external field and magnetization of the ferromagnetic clusters. The magnetization produced by the nano-clusters is the sum of an averaged magnetization $4\pi\mathbf{M}$ and a random magnetic field $\mathbf{h}(\mathbf{r})$ with zero average value. According to our experimental data, the magnetic moments of the clusters are practically parallel to the applied magnetic field if $H \gtrsim 10$ Oe. Thus, the induction $\mathbf{B} = \mathbf{H} + 4\pi\mathbf{M} + \mathbf{h}(\mathbf{r}) = \overline{\mathbf{B}} + \mathbf{h}(\mathbf{r})$ has only a transverse component in the transverse applied field $H > 10$ Oe. Under this condition we can calculate the averaged square of $\mathbf{h}(\mathbf{r})$ using the Wiener–Khinchin theorem and having in mind that $d \sim l_g \gg r_g$. We obtain the practically evident result after standard calculations

$$\langle \mathbf{h}^2 \rangle = \frac{1}{V} \int \mathrm{d}\mathbf{r} h^2(\mathbf{r}) = M^2, \tag{1}$$

where V is the sample volume.

The induction $\mathbf{B}$ is an external transverse magnetic field for the Nb film, which penetrates the superconductor and generates a lattice of Abrikosov vortices. The thickness of the superconducting film is less than the London penetration depth in Nb, $\lambda \approx 200$ nm. The external field is transverse and not small. Then, the average inductions in Nb and $Pd_{0.99}Fe_{0.01}$ films are equal.

The vortex lattice occupies a position with the minimum Gibbs magnetic energy U_m. This energy can be expressed as

$$U_m(\mathbf{b}_f) = \frac{1}{4\pi V} \int_V \mathrm{d}\mathbf{r} \left[\frac{(\overline{\mathbf{B}} + \mathbf{b}_f)^2}{2} - (\overline{\mathbf{B}} + \mathbf{h})(\overline{\mathbf{B}} + \mathbf{b}_f) \right], \tag{2}$$

where $\mathbf{b}_f$ is the perturbation of the magnetic induction due to strain of the vortex lattice in the non-uniform external field. The average of $\mathbf{b}_f$ over the volume V is zero. The additional pinning energy due to the vortex redistribution is $U_p = U_m(\mathbf{b}_f) - U_m(0)$. The value of $\mathbf{b}_f$ is determined by the condition of the minimum of the Gibbs energy, $\delta U_m(\mathbf{b}_f)/\delta \mathbf{b}_f = 0$. From the latter condition and equation (2), we readily obtain that $\mathbf{b}_f = \mathbf{h}$ and

$$U_p = -\frac{\langle \mathbf{h}^2 \rangle}{8\pi}. \tag{3}$$

The function $h(\mathbf{r})$ has two characteristic lengths, the size of the magnetic clusters and the distance between them. The characteristic scale of the pinning potential is evidently of the order of the distance between the magnetic clusters l_g. Thus, the increase of the critical current density Δj_c can be obtained from the balance of the Lorentz $B_f \Delta j_c / c$ and pinning U_p / l_g forces. As a result, we have

$$\Delta j_c = \frac{c \langle h^2 \rangle}{8\pi B_f l_g}. \tag{4}$$

Using equation (1), we derive a final estimate for the increase of the critical current density due to inhomogeneity of the ferromagnetic layer in the form

$$\Delta j_c = \frac{cM^2}{8\pi l_g (H + 4\pi M)}. \tag{5}$$

Substituting in equation (5) the magnetization $M = 20\,\mathrm{emu\,cm^{-3}}$, $l_g = 100$ nm, and $H = 20$ Oe we get $\Delta j_c \approx 10^5\,\mathrm{A\,cm^{-2}}$, which is approximately 25% of j_c in the Nb film measured by the four-probe method. This estimate is also in agreement with the MO data (figure 5).

5. Conclusions

We study magnetic and superconducting characteristics of the ferromagnetic–superconducting heterostructure $Pd_{0.99}Fe_{0.01}$–Nb. We show that the properties of the $Pd_{0.99}Fe_{0.01}$ thin films are characteristic of nano-cluster systems. The estimated value of the magnetic moment per Fe ion is about 3.7 μ_B, which is close to the 4 μ_B characteristic of Pd_3Fe alloy. We also estimate the size of the magnetic clusters, $r_g \sim 10$ nm, and the distance between them, $l_g \sim 100$ nm. The inhomogeneous magnetic structure of the $Pd_{0.99}Fe_{0.01}$ layer gives rise to a considerable increase of the critical current density in the Nb film. At the same time, $Pd_{0.99}Fe_{0.01}$ film is shown to be a magnetically soft nano-clustered material, so one can expect a high rate of dynamic magnetization reversal. Therefore, the nano-cluster structure of $Pd_{0.99}Fe_{0.01}$ thin films is favorable for applications in devices based on SFS junctions.

Acknowledgments

The work is supported by the Russian Foundation for Basic Research (projects no 12–02-00339 and no 12–02-00707).

References

[1] Kupriyanov M Y, Golubov A A and Sigel M 2006 *Proc. SPIE* **6260** 62600S

[2] Vernik I V, Bol'ginov V V, Bakurskiy S V, Golubov A A, Kupriyanov M Y, Ryazanov V V and Mukhanov O A 2013 *IEEE Trans. Appl. Supercond.* **23** 1701208

[3] Larkin T I, Bol'ginov V V, Stolyarov V S, Ryazanov V V, Vernik I V, Tolpygo S K and Mukhanov O A 2012 *Appl. Phys. Lett.* **100** 222601

[4] Schöck M, Sürgers C and von Löhneysen H 2000 *Eur. Phys. J.* B **14** 1

[5] Ryazanov V V, Oboznov V A, Veretennikov A V and Rusanov A Y 2001 *Phys. Rev.* B **65** 020501

[6] Andreev A V, Buzdin A I and Osgood R M 1991 *Phys. Rev.* B **43** 10124

[7] Bol'ginov V V, Stolyarov V S, Sobanin D S, Karpovich A L and Ryazanov V V 2012 *JETP Lett.* **95** 366

[8] Chepulskii R V, Barabash S V and Zunger A 2012 *Phys. Rev.* B **85** 144201

[9] Kudrnovský J, Drchal V, Khmelevskyi S and Turek I 2011 *Phys. Rev.* B **84** 214436

[10] Skomski R, Kashyap A, Solanki A, Enders A and Sellmyer D J 2010 *J. Appl. Phys.* **107** 09A735

[11] Parra R E and Gonzalez A C 1996 *J. Appl. Phys.* **79** 5242

[12] Kondo Y, Swieca K and Pobell F 1995 *J. Low Temp. Phys.* **100** 195

[13] Wang Z, Kunkel H P and Williams G 1993 *J. Appl. Phys.* **73** 5674

[14] Crangle J and Scott W R 1965 *J. Appl. Phys.* **36** 921

[15] Salikhov R I, Garifullin I A, Garif'yanov N N, Tagirov L R, Theis-Brühl K, Westerholt K and Zabel H 2009 *Phys. Rev. Lett.* **102** 087003

[16] Papaefthymiou G C, Bryden K J and Ying J Y 2002 *Physica B: Cond. Mat.* **311** 279

[17] Bergmann G 1978 *Phys. Rev. Lett.* **41** 264

[18] Berger L and Bergmann G 1980 The Hall Effect and Its Applications ed C L Chien and C R Westgate (New York: Plenum)

[19] Kontos T, Aprili M, Lesueur J and Grison X 2001 *Phys. Rev. Lett.* **86** 304

[20] Nagaosa N, Sinova J, Onoda S, MacDonald A H and Ong N P 2010 *Rev. Mod. Phys.* **82** 1539

[21] Karplus R and Luttinger J M 1954 *Phys. Rev.* **95** 1154

[22] Uspenskaya L S, Tikhomirov O A, Bozhko S I, Egorov S V and Chugunov A A 2013 *J. Appl. Phys.* **113** 163907

[23] Jooss C, Albrecht J, Kuhn H, Leonhardt S and Kronmüller H 2002 *Rep. Prog. Phys.* **65** 651

[24] Khapikov A, Uspenskaya L, Ebothe J and Vilain S 1998 *Phys. Rev.* B **57** 14990

[25] Baykal A, Karaoglu E, Sözeri H, Uysal E and Toprak M 2013 *J. Supercond. Nov. Magn.* **26** 165

[26] Heller B *et al* 1998 *J. Nucl. Instr. and Meth. in Phys. Res.* B **142** 133

[27] Coey J M D 2010 *Magnetism and Magnetic Materials* (New York: Cambridge University Press)
[28] Shinohara T, Sato T, Taniyama T and Nakatani I 1999 *J. Magn. Magn. Mat.* **196-197** 94
[29] Uspenskaya L S, Rakhmanov A L, Dorosinskii L A, Chugunov A A, Stolyarov V S, Skryabina O V and Egorov S V 2013 *JETP Lett.* **97** 155